論文 / 著書情報
Article / Book Information

Title	Observation of emission process in hydrogen-like nitrogen Z-pinch discharge with time integrated soft X-ray spectrum pinhole image
Authors	Y. Sakai,J. Rosenzweig,H. Kumai,Y. Nakanishi,Y. Ishizuka,S. Takahashi,T. Komatsu,Y. Xiao,H. Bin,Z. Qiushi,Y. Hayashi,I. Song,T. Kawamura,M. Watanabe,E. Hotta
Citation	Physics of Plasmas, Vol. 20, ,
Pub. date	2013, 2
URL	http://scitation.aip.org/content/aip/journal/pop
Copyright	Copyright (c) 2013 American Institute of Physics

Observation of emission process in hydrogen-like nitrogen Z-pinch discharge with time integrated soft X-ray spectrum pinhole image

Y. Sakai, J. Rosenzweig, H. Kumai, Y. Nakanishi, Y. Ishizuka et al.

Citation: Phys. Plasmas **20**, 023108 (2013); doi: 10.1063/1.4789617
View online: http://dx.doi.org/10.1063/1.4789617
View Table of Contents: http://pop.aip.org/resource/1/PHPAEN/v20/i2
Published by the American Institute of Physics.

Observation of emission process in hydrogen-like nitrogen Z-pinch discharge with time integrated soft X-ray spectrum pinhole image

Y. Sakai,[1,a)] J. Rosenzweig,[2] H. Kumai,[1] Y. Nakanishi,[1] Y. Ishizuka,[1] S. Takahashi,[1] T. Komatsu,[1] Y. Xiao,[1] H. Bin,[1] Z. Quishi,[1] Y. Hayashi,[1] I. Song,[1] T. Kawamura,[1] M. Watanabe,[1] and E. Hotta[1]

[1]*Department of Energy Sciences, Tokyo Institute of Technology, Nagatsuta, Midoriku, Yokohama, Kanagawa 226-8502, Japan*

[2]*Department of Physics and Astronomy, University of California Los Angeles, 405 Hilgard Ave., Los Angeles, California 90095, USA*

(Received 25 July 2012; accepted 11 January 2013; published online 28 February 2013)

The emission spectra of hydrogen-like nitrogen Balmer at the wavelength of 13.4 nm in capillary Z-pinch discharge plasma are experimentally examined. Ionization to fully strip nitrogen at the pinch maximum, and subsequent rapid expansion cooling are required to establish the population inversion between the principal quantum number of $n=2$ and $n=3$. The ionization and recombination processes with estimated plasma parameters are evaluated by utilizing a time integrated spectrum pinhole image containing radial spatial information. A cylindrical capillary plasma is pinched by a triangular pulsed current with peak amplitude of 50 kA and pulse width of 50 ns. © *2013 American Institute of Physics*. [http://dx.doi.org/10.1063/1.4789617]

I. INTRODUCTION

Soft X-ray lasers (SXRLs) in hot plasma have been investigated for a few decades by now,[1] following the lasing process pumped by irradiation of pulsed laser to a solid medium.[2–6] In a high energy density plasma, where radiation diverges significantly, several unique schemes are utilized in order to elongate the amplification path, such as capillary ablative wave guiding,[3] curved targets,[7] pulsed train lasers[8] or grazing incidence irradiation.[9] In 1994, lasing of a Ne-like Ar collisional SXRL at an wavelength of 46.9 nm has been demonstrated by use of a capillary Z-pinch gas discharge,[10] which realizes higher energy conversion efficiency and stable repetitive operation.[11–13] In these experiments, a predischarge has been employed to suppress the MHD instability growth in the implosion phase, and use of the gaseous medium makes it possible to optimize an initial discharge condition.[14] Meanwhile, the possibility of SXRL at shorter wavelengths has also been investigated resulting in the lasing at 13.2 nm Ni-like Cd and 18.2 nm H-like C recombination lines by ablative capillary discharge.[15–19] As a consequence, a gas discharge H-like N recombination SXRL (Fig. 1) at the wavelength of 13.4 nm (EUV) has been proposed,[20] and the observation of He and Lyman series radiation has been reported thus far.[21,22]

Lasing of the Balmer α radiation requires a strong ionization, to NVIII at the maximum pinch, and subsequent rapid cooling. These requirements are needed to establish the population inversion between the principal quantum number $n=2$ and $n=3$; the population of the ground state should be low enough to suppress radiation trapping by the Ly α, besides collisional or radiative de-excitation rates from the higher states to $n=3$ state should be higher than the radiative decay rate from $n=3$ to lower states, while collisional excitation from the ground state to $n=2$ state should be suppressed. In this paper, experimental observation of the Balmer, Lyman series and He-like resonance lines using a time integrated spectrum pinhole images (Fig. 2) are reported. The ionization and recombination process of nitrogen discharge are investigated for insight into the formation of the population inversion.

II. EXPERIMENTAL DESCRIPTION

H-like N plasma was generated by a triangular pulsed current having a peak amplitude of 50 kA and a pulse width of 50 ns.[23,24] An alumina (Al_2O_3) ceramic capillary with an inner radius of 1.5 mm and a length of 75 mm was filled with nitrogen molecular gas at differing initial pressures P_{ini} (estimated from the initial NII number density N^{+1} at the room temperature) of about 2500 mTorr ($N^{+1} \sim 1.5\times10^{17}\,cm^{-3}$), 1500 mTorr ($N^{+1} \sim 1.0\times10^{17}\,cm^{-3}$), 1000 mTorr ($N^{+1} \sim 6.5\times10^{16}\,cm^{-3}$), 750 mTorr ($N^{+1} \sim 5.0\times10^{16}\,cm^{-3}$), and 250 mTorr ($N^{+1} \sim 1.5\times10^{16}\,cm^{-3}$). Nitrogen gas was slowly pre-ionized[11] by a small RC circuit-derived current with an amplitude of 10 A, and a decay time constant of 3 μs. A schematic diagram of the time-integrated spectrum pinhole imaging set-up is shown in Fig. 2. The spectrum of the nitrogen plasma was resolved using a transmission grating with a lattice constant of 1/1000 mm^{-1}, in combination with

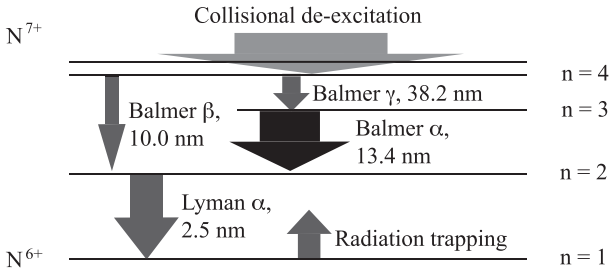

FIG. 1. Quantum levels of H-like N ion.

[a)]Present affiliation: Department of Physics and Astronomy, UCLA, 405 Hilgard Ave., Los Angeles, California 90095, USA.

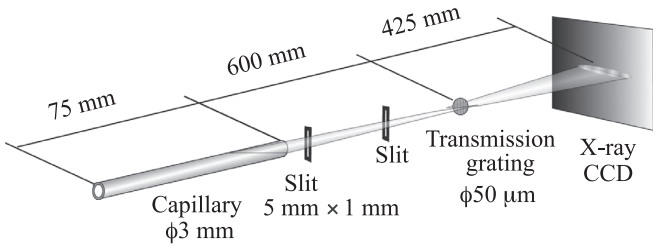

FIG. 2. Time integrated spectrum pinhole imaging set-up.

an X-ray CCD camera (Andor DO434) that has 1024 × 1024 pixels with each pixel area of 13-μm square. The transmission grating was placed at a distance of 600 mm from the end of the capillary, and a distance between the grating and the CCD camera was 425 mm. Two slits of 1 mm × 5 mm were placed between the capillary and the transmission grating. The aperture diameter of the transmission grating was 50 μm. For 10 nm soft X-rays, the spectral resolution is ~0.2 nm with $\Delta\lambda/\lambda \sim 1/50$, and the radial (vertical) spatial resolution is ~10 μm.

The local electron temperature of the highly-charged nitrogen plasma is estimated by fitting the temperature-slope of the bremsstrahlung radiation formula,[25,26]

$$P_{\mathrm{ff}} \propto n_{\mathrm{e}} N_{\mathrm{i}} \sqrt{T_{\mathrm{e}}} \left(\frac{Z_{\mathrm{ave}}}{\sqrt{T_{\mathrm{e}}}} \right)^2 \exp\left(-\frac{\hbar\omega}{T_{\mathrm{e}}} \right). \quad (1)$$

where, Z_{ave} is an average charge state number, $\hbar$ is the reduced Planck constant, ω is the angular frequency, T_{e} is the electron temperature, N_{i} and n_{e} are the ion and electron densities, respectively. In the Z-pinch discharge, electron temperature satisfies $T_{\mathrm{e}} < \hbar\omega$ for the Balmer and Lyman series. Thus, the bremsstrahlung radiation formula is approximately reduced to an exponential factor. The electron temperature is roughly estimated in the order of 25 eV, as one physical reference of the anisotropic ionization non-equilibrium plasma. It should be noted that the ablated material (mainly oxygen), which is also considered in the interpretation of the spectra, may not be evenly distributed at the beginning of main discharge. Therefore, the spectra of the H-like oxygen ions are significant when the initial nitrogen gas pressure is 250 mTorr. Each spectrum is taken by a single shot, and the reproducibility is relatively high as long as proper pre-discharge current is measured, as is shown in Ref. 11.

III. RESULTS

Typical observed spectrum pinhole images are shown in Fig. 3. In the Z-pinch plasma, ionization to the NVI state only proceeds in the implosion phase at a temperature in the range of several tens of eV. Afterward, the transition to NVII and NVIII states proceeds. Strong emission of the He α line of NVI at the wavelength of approximately 3 nm has been observed on capillary axis. In contrast, NVII and NVIII are generated at the maximum pinch, which remain in the subsequent expansion phase. Therefore, the Balmer series of NVII at a wavelength of several nm may be observed near the upper and lower edge (off-axis) of the spectrum pinhole

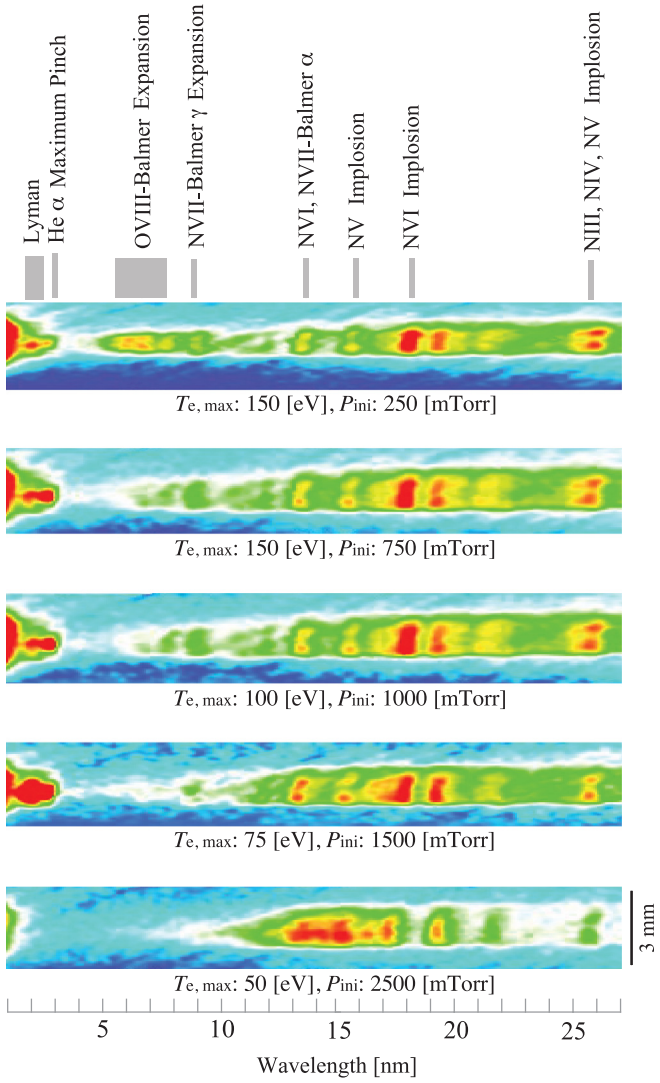

FIG. 3. Typical observed time integrated spectrum pinhole images at various initial N_2 gas pressures.

images. Hence the plasma parameters at the maximum pinch are evaluated using the on-axis profiles, where emission intensity is strongest. The off-axis spectrum profiles containing the Balmer series radiation are used to give information on the expansion phase.

It should be noted that the on-axis slope of the temperature curve are more or less affected by the implosion and expansion phase, which lowers the estimated T_{e} at the maximum pinch. However, although the total soft-X-ray radiation measured by the XRD at the maximum pinch and in the expansion phase are about the same intensity, strong emission from the He and Lyman series only exists at the maximum pinch.[22] As shown in the following experimental results, the observed minimum radius of the pinched plasma is approximately <1/5 of the capillary inner radius, and therefore the photon density in the expansion phase is decreased by one order of magnitude. Thus, the on-axis spectrum is used to evaluate the plasma parameters at the maximum pinch. Typically, a secondary pinch was not observed and maximum pinch occurs in the first decay phase of the triangular pulsed current, as shown in typical XRD signals.[22,27] However, in the experiment with initial gas

pressure of 250 mTorr, a secondary pinch or slow expansion after the first maximum pinch might have occurred.

A. Maximum pinch

On-axis spectrum profiles for various initial gas pressures at the wavelength of below 15 nm are shown in Fig. 4(Left). Local electron temperatures are estimated as represented in Fig. 4(Right) using the continuous spectrum at a wavelength of around hundreds of eV. The correlation between the estimated $T_{e,max}$ and ionic charge state at the maximum pinch is analyzed as follows:

(a) $P_{ini} = 2500$ mTorr, $T_{e,max} \sim 50$ eV
The estimated electron temperature is ~50 eV and H-like N line is not observed.

(b) $P_{ini} = 1500$ mTorr, $T_{e,max} \sim 75$ eV
$T_{e,max}$ is increased to about ~75 eV and He α at a wavelength of around 3 nm are observed. Weak radiation at a wavelength of 13–14 nm is observed that is considered to be mainly emitted from the NVI state.

(c) $P_{ini} = 1000$ mTorr, $T_{e,max} \sim 100$ eV
Discrete line spectra in the wavelength of <10 nm are observed at $T_{e,max} \sim 100$ eV. Therefore, Balmer series radiation of NVII and OVIII lines is confirmed. Weak radiation in the wavelength range of 6–8 nm corresponds to the Balmer series of OVIII.

(d) $P_{ini} = 750$ mTorr, $T_{e,max} \sim 150$ eV
The electron temperature is increased to $T_{e,max} \sim 150$ eV, resulting in observed enhancement of the He lines and Lyman series. Thus, highly excited states of H-like N ion are generated, and therefore the existence of NVIII is expected.

(e) $P_{ini} = 250$ mTorr, $T_{e,max} \sim 150$ eV
The maximum temperature may saturate at $T_{e,max} \sim 150$ eV. In this case, intensity of the Balmer series of OVIII at a wavelength of about 6–8 nm is significantly enhanced, which indicates an increase of ablation materials from the inner wall of the Al_2O ceramic capillary. Strong continuum radiation at wavelengths <7 nm implies the existence of the NVIII as well as OVIIII. Large amount of the ablation materials may decrease the maximum temperature by insufficient compression or strong radiation cooling by O and Al.

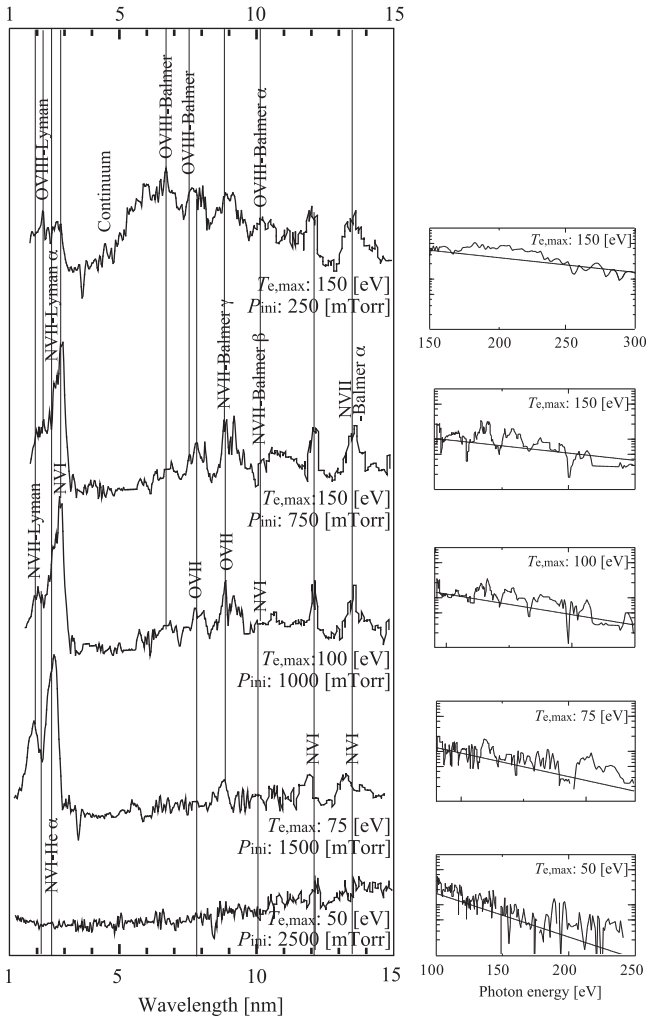

FIG. 4. (Left) On-axis emission spectrum profiles at various initial gas pressures. These spectra are expected to have the information at the maximum pinch. (Right) Estimated on-axis local electron temperature obtained by fitting a spectrum profile at around hundreds of eV to bremsstrahlung free-free radiation intensity formula.

As a result, emission of Balmer series as well as Lyman series has been observed with an estimated temperature of 100–150 eV. A relatively shorter pulse width of discharge current makes it possible to pinch the plasma column without significant ablation of the capillary inner wall.[21] From Fig. 3 in the case of initial gas pressure of 750, 1000, and 1500 mTorr, strong intensity of He α radiation is observed, with a plasma radius in the range of a few hundreds of μm. The He α radiation is thought to be emitted at the implosion and the maximum pinch. It should be noted that this strong radiation could be utilized as a compact radiation source in the water window regime, as proposed in Ref. 28.

The FWHM of He α line shown in Fig. 5 is approximately 1/5 of capillary inner radius. Assuming that nitrogen plasma is fully ionized to NVI or higher charge states at the maximum pinch, the maximum n_e is approximately estimated as

$$n_{e,max} \sim Z_{ave} N^{+1} \left(\frac{r_{ini}}{r_{min}}\right)^2 \sim 10^{19} \ [\mathrm{cm}^{-3}], \qquad (2)$$

where the average charge state number is assumed to be $Z_{ave} \sim 5$, and the initial number density is $N^{+1} \sim 5 \times 10^{16}\,\mathrm{cm}^{-3}$.

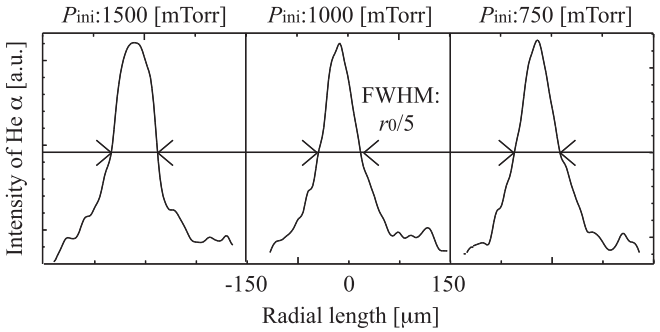

FIG. 5. Intensity profiles of He α line at a wavelength of around 3 nm with an initial nitrogen gas pressure of 1500, 1000, and 750 mTorr.

B. Expansion phase

The plasma parameters in the expansion phase are evaluated from the off-axis spectrum in the wavelength range of several nm. The estimated electron temperature and electron number density at radial positions of 0-200 μm, 400–600 μm, and 800–1000 μm for initial gas pressures of 1500 mTorr, 750 mTorr, and 250 mTorr are shown in Fig. 6.

(a) $P_{\mathrm{ini}} = 1500$ mTorr, $T_{\mathrm{e,max}} \sim 100$ eV
The estimated maximum temperature (on-axis) is $T_{\mathrm{e,max}} \sim 100$ eV and off-axis electron temperature decreases to ~50 eV. Since ionization to NVII and NVIII states are not sufficient, Balmar series is not observed in any radial position.

(b) $P_{\mathrm{ini}} = 750$ mTorr, $T_{\mathrm{e,max}} \sim 150$ eV
It is expected that the pinched plasma with a radius of ~200 μm, $T_{\mathrm{e,max}} \sim 150$ eV, and $n_{\mathrm{e}} \sim 10^{19}\,\mathrm{cm}^{-3}$ expands to a radius of ~400–600 μm and cooled down to ~75 eV with $n_{\mathrm{e}} \sim 10^{18}\,\mathrm{cm}^{-3}$. At a radius of ~800–1000 μm, the estimated temperature is further decreased to ~50 eV. In the off-axis position, with an estimated temperature of ~75 eV, a slight enhancement of the relative intensity of the Balmer series radiation with respect to the NVI line at the wavelength of 12 nm is observed. Also, enhancement of the emission intensity at the tail of the Balmer series may suggest the existence of the satellite lines by doubly excited states. These results may be revealing the presence of the enhanced stimulated emission of Balmer series in the expansion phase. The intensity ratios of the Balmer α, γ to the NVI line for on-axis and off-axis position are 1:1 and 2:1, respectively.

(c) $P_{\mathrm{ini}} = 250$ mTorr, $T_{\mathrm{e,max}} \sim 150$ eV
Relative slight enhancement of Balmer series is observed in the off-axis region. Although the pinched plasma with $T_{\mathrm{e,max}} \sim 150$ eV may cooled down to ~75 eV when a plasma radius is about 400–600 μm, the temperature at a radius of about 800–1000 μm does not drop to <75 eV. This may be caused by an additional heating after the first maximum pinch, due to the mismatching between shorter pinch time and the phase of triangular pulsed current.

IV. DISCUSSION

In order to establish the population inversion in Balmer α, requirements for the transition rate of $n = 2$ and $n = 3$ states are evaluated by

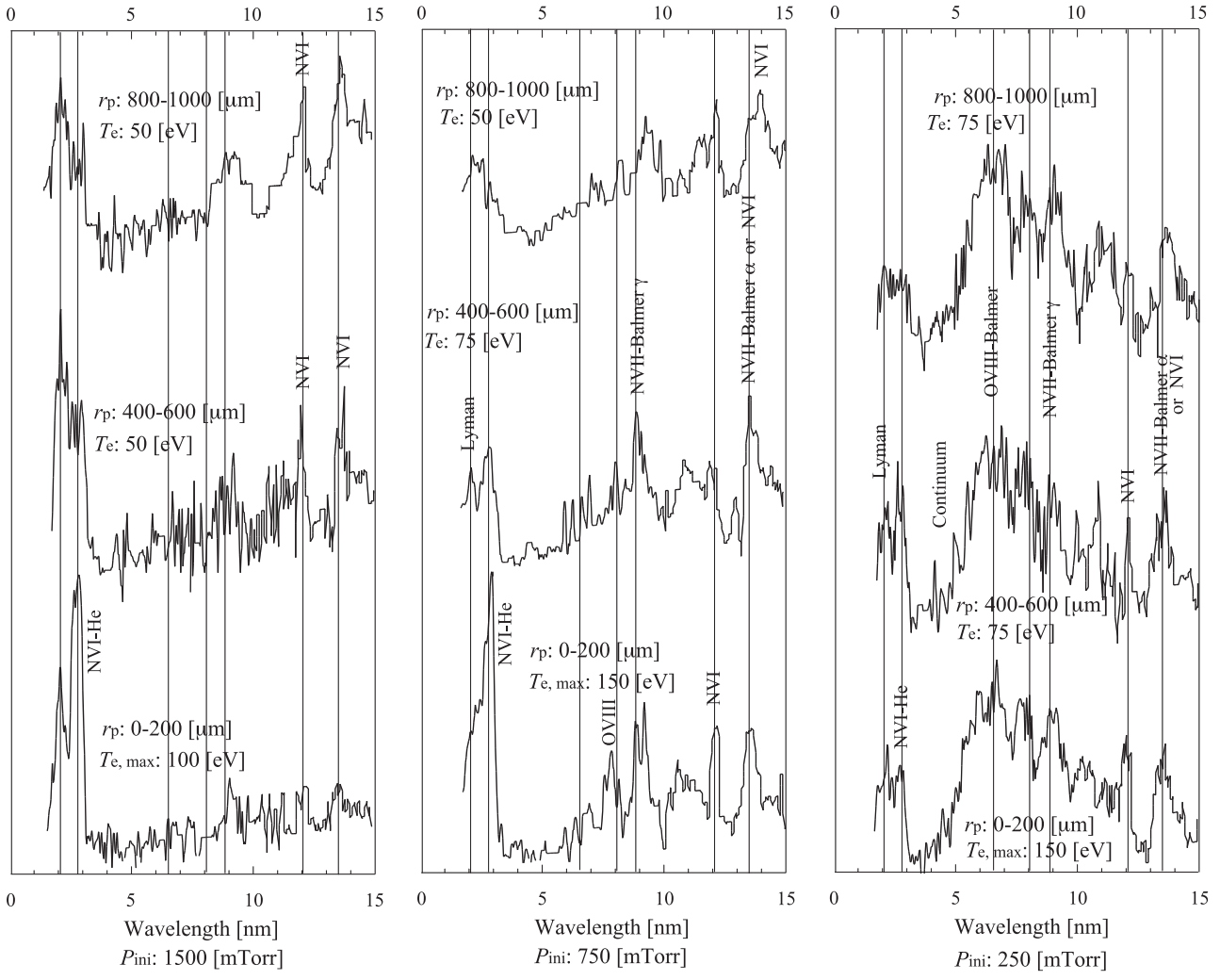

FIG. 6. Off-axis spectrum profiles at various initial gas pressures, which are expected to have information in the expansion phase.

$$\frac{dN^{+6}_{n=3}}{dt} > \frac{dN^{+6}_{n=2}}{dt} \quad . \tag{3}$$

From the spectrum, pinhole images in the expansion phase of the initial gas pressure of 750 mTorr, the estimated n_e is in the order of $10^{18}\,cm^{-3}$ with $T_e \sim 50$–$75\,eV$. In this case, collisional relaxation time $\tau_{LTE,p-q}$ between quantum levels p and q is several ns for $n=4$ and $n=5$ states, and is increased by one order of magnitude for the $n=3$ and $n=4$ states, which may be evaluated by collisional de-excitation rate coefficient $DE_{p\text{-}q}$ given as,[25,29]

$$\tau_{LTE,p-q} \sim \frac{1}{DE_{p-q}(T_e)n_e}. \tag{4}$$

Thus, Griem's boundary is estimated to be in the range $n=3$–4 when the expanding plasma reaches inner wall of the capillary and collisional excitation from $n=2$ to $n=3$ states is suppressed. In this condition, the transition rates of $n=2$ and $n=3$ can be evaluated using the escape factor Λ expressed as

$$\left.\begin{aligned}\frac{dN^{+6}_{n=3}}{dt} &\sim n_e N^{+6}_{n=4} DE_{\ 4-3}(T_e) - N^{+6}_{n=3}(A_{n=3-2}+A_{n=3-1})\\ \frac{dN^{+6}_{n=2}}{dt} &\sim N^{+6}_{n=3}A_{n=3-2} - N^{+6}_{n=2}\Lambda_{n=2-1}A_{n=2-1}\end{aligned}\right\}. \tag{5}$$

Therefore, approximately the inequality Eq. (3) leads to a sufficient condition for the escape factor given by

$$\begin{aligned}&\frac{N^{+6}_{n=3}(2A_{n=3-2}+A_{n=3-1}) - n_e N^{+6}_{n=4} DE_{\ 4-3}(T_e)}{N^{+6}_{n=2}A_{n=2-1}}\\ &< \frac{N^{+6}_{n=3}}{N^{+6}_{n=2}}\frac{2A_{n=3-2}+A_{n=3-1}}{A_{n=2-1}} \sim \frac{2A_{n=3-2}+A_{n=3-1}}{A_{n=2-1}}\\ &\sim \frac{1}{2} < \Lambda_{2p-1s},\end{aligned} \tag{6}$$

as long as the plasma of NVIII state is in the recombination phase. In a highly charged H-like N plasma, the escape factor Λ is affected by several phenomenon, such as Stark and impact broadening,[25] thus detailed numerical analysis should be required. However, in this discussion, the escape factor may be analytically evaluated from Eq. (6) by only taking into account the Doppler shift. The escape factor Λ for Gaussian profile due to the Doppler shift in a cylindrical plasma column is approximated as[1,26,30]

$$\left.\begin{aligned}\Lambda &\sim \frac{1}{\overline{\tau}(\pi \log \overline{\tau})^{1/2}},\\ \overline{\tau} &\sim \sqrt{\pi}\ \overline{N}_l l \frac{e^2}{m_e c} f_{u-l}\frac{h}{\Delta\hbar\omega},\end{aligned}\right\} \tag{7}$$

where N_l is the number density of lower level, l is the effective length of light pass, and f_{u-l} is the oscillator strength. In the Z-pinch discharge, the radial gradient of fluid velocity is presumed to reach $\nabla v_{Fluid} \sim 10^5/s$ in the expansion phase.[22] Thus, the Doppler shift of the angular frequency associated with the fluid motion is several times larger than that arising from thermal effects.[1,31] Using the expanding plasma radius of several hundreds of μm as the characteristic plasma length, $\Lambda_{n=1-2} > 1/2$ yields a required ion number density of $N^{+6}_{n=1} < 10^{16\text{–}17}\,cm^{-3}$.

Consequently, a fully stripped nitrogen plasma is necessary, and this requirement could not be satisfied in the experiment, as evaluated in the following discussion. In the experiment, $n_{e,max} \sim 10^{19}\,cm^{-3}$, $N^{+6}_{n=1} \sim 10^{18}\,cm^{-3}$, and $T_{e,max} \sim 150\,eV$ are considered to be obtained at the maximum pinch. In addition, from the time evolution of XRD signal,[22] the maximum pinch duration is estimated to be $\Delta t_{max} \sim$ several ns. Assuming that almost all of NVII is ionized to H-like N ions at the beginning of the maximum pinch, N^{+7} is estimated to be less than half of N^{+6}, as

$$\begin{aligned}N^{+7} &\sim \int \mathcal{J}(T_e) n_e N^{+6} dt \sim \mathcal{J}(T_{e\ max}) n_{e,max} N^{+6} \Delta t_{max}\\ &< \frac{1}{2}N^{+6},\end{aligned} \tag{8}$$

where $\mathcal{J}(T_e)$ is Seaton's collisional ionization rate coefficient,

$$\mathcal{J}(T_e) \sim 2\times 10^{-6}\frac{1}{\sqrt{T_e[eV]}}\frac{1}{|\Delta E_{ion}|}\exp\left(\frac{-|\Delta E_{ion}|}{T_e}\right)\ [cm^3/s], \tag{9}$$

which is a function of T_e and ionization potential ΔE_{ion}.[25,26,32] In this experiment, $N^{+6}_{n=1}$ is estimated to be in the order of $10^{18}\,cm^{-3}$ at the maximum pinch, and $10^{17}\,cm^{-3}$ when the plasma is cooled down to a several tens of eV. Therefore, the required sufficient condition $N^{+6}_{n=1} < 10^{16\text{–}17}$ could not be satisfied in the experiment, and further increase of energy density for stronger ionization is necessary to avoid radiation trapping.

Assuming that the Griem's boundary is between $n=3$ and 4, if the supply of the population from the continuum state to $n=4$ state by collisional de-excitation is large enough, the population of $n=3$ state could be sufficient for the formation of population inversion with respect to the $n=2$ state. Thus, the requirement for the collisional de-excitation is reduced to

$$DE_{n=5-4} n_e > A_{n=4-3} \sim 10^{10}\ [s^{-1}]. \tag{10}$$

As a result, the electron number density of $n_e \sim 10^{18}\,cm^{-3}$ requires electron temperature of a few tens of eV. In order to ionize NVII to NVIII state by a factor of several times higher, $n_{e,\ max}$ should be increased by one order or $T_{e,max}$ should be $>200\,eV$ with $\mathcal{J}(200\ [eV])/\mathcal{J}(150[eV]) \sim 10$ for rapid ionization in the maximum pinch using only several ns. However, the increase of n_e by one order of magnitude also shortens the collisional thermalization time for the $n=3$ state to ns order. Technically, it is difficult to cool down the discharge plasma from $T_{e,max} \sim 150\,eV$ to a few tens of eV in a few ns, hence the increase of n_e should be considered carefully.

On the other hand, increase of $T_{e,max}$ to ~200 eV also increases the $T_{e,cooled}$ in the expansion phase. However, the increase of $T_{e,max}$ from 150 eV to 200 eV would not significantly affect the cooling time, because the free expansion time scale is on the order of several ns to a few tens of ns as long as the discharge current decays sufficiently quickly.[22] Even the radiation cooling removes the excess heat energy of 50 eV within a few tens of ns by radiative recombination according to the following:

$$50\,[\mathrm{eV}] \sim \frac{\int_{t_{200[\mathrm{eV}]}}^{t_{150[\mathrm{eV}]}} \int_0^{\infty} \{n_e N^{+7} R_{rad}(T_e)\} T_e dT_e dt}{n_e + N^{+7}}, \sim \frac{n_e N^{+7} R_{rad}(100\ [\mathrm{eV}]) \times \mathrm{a\ few\ tens\ [ns]}}{n_e + N^{+7}} \times 100\ [\mathrm{eV}], \quad (11)$$

where $R_{rad}(T_e)$ is the radiative recombination rate coefficient.[27] Thus, the increase of $T_{e,max}$ to ~200 eV would be preferred for stronger ionization to NVIII.

V. CONCLUSIONS

The emission spectra of H-like N plasma was analyzed using the time integrated spectrum pinhole image. H-like N ions are generated at the estimated temperature of >100 eV, and the existence of NVIII state is anticipated at $T_{e,max} \sim 150$ eV with $n_{e,\,max} \sim 10^{19}\,\mathrm{cm}^{-3}$. The Balmer series observed in the off-axis spectrum profiles are expected to have information on the recombination phase with estimated electron temperature of ~50–75 eV. However, T_e and n_e at the maximum pinch are not sufficiently high to strongly ionize NVII to the NVIII state. Thus, further experimental investigation of the ionization and recombination dynamics with $T_{e,max} \sim 200$ eV would be necessary in this approach. Also, further numerical investigation of the detailed recombination kinetics[33] is needed. However, the feasibility of H-like N discharge plasma as a compact soft X-ray source using Balmer, He, and Lyman series radiation is shown.

ACKNOWLEDGMENTS

The authors would like to thank the invaluable advice of all of the members in Department of Energy Sciences, Tokyo Institute of Technology. Also, we would like to acknowledge the Seimitsu Kosaku Gijutsu Center of Tokyo Institute of Technology, Murata Co., Ltd., Takatsuki Musen Co., Ltd., Fuji Vacuum Co., Ltd., and USHIO Inc. for their help in construction of high voltage pulsed power device in Tokyo Institute of Technology.

This work supported by mainly the Japan Society for the Promotion of Science, and partially U.S. Department of Energy under Contracts No. DE-FG02-07ER46272, No. DE-FG03-92ER40693, the Office of Naval Research under Contract No. ONR N00014-06-1-0925, Defense Threat Reduction Agency Contract No. HDTRA1-10-1-0073, and DARPA under Contract No. N66001-11-1-4197.

[1]R. C. Elton, *X-ray Lasers* (Academic Inc., USA, 1990).
[2]D. L. Matthews, P. L. Hagelstein, M. D. Rosen, M. J. Eckart, N. M. Ceglio, A. U. Hazi, H. Medecki, B. J. MacGowan, J. E. Trebes, B. L. Whitten, E. M. Campbell, C. W. Hatcher, A. M. Hawryluk, R. L. Kauffman, L. D. Pleasance, G. Rambach, J. H. Scofield, G. Stone, and T. A. Weaver, Phys. Rev. Lett. **54**, 110 (1985).
[3]S. Suckewer, C. H. Skinner, H. Milchberg, C. Keane, and D. Voorhees, Phys. Rev. Lett. **55**, 1753 (1985).
[4]P. V. Nickles, V. N. Shlyaptsev, M. Kalachnikov, M. Schnürer, I. Will, and W. Sandner, Phys. Rev. Lett. **78**, 2748 (1997).
[5]R. Smith, G. J. Tallents, J. Zhang, G. Eker, S. McCabe, G. J. Pert, and E. Wolfrum, Phys. Rev. A **59**, R47 (1999).
[6]T. Kawachi, A. Sasaki, M. Tanaka, M. Kishimoto, N. Hasegawa, K. Nagashima, M. Koike, H. Daido, and Y. Kato, Phys. Rev. A **69**, 033805 (2004).
[7]R. Kodama, D. Neely, Y. Kato, H. Daido, K. Murai, G. Yuan, A. MacPhee, and C. L. S. Lewis, Phys. Rev. Lett. **73**, 3215 (1994).
[8]H. Daido, Y. Kato, K. Murai, S. Ninomiya, R. Kodama, G. Yuan, Y. Oshikane, M. Takagi, H. Takbe, and F. Koike, Phys. Rev. Lett. **75**, 1074 (1995).
[9]Y. Wang, M. A. Larotonda, B. M. Luther, D. Alessi, M. Berrill, V. N. Shlyaptsev, and J. J. Rocca, Phys. Rev. A **72**(5), 053807 (2005).
[10]J. J. Rocca, V. Shlyaptsev, F. G. Tomasel, O. D. Cortázar, D. Hartshorn, and J. L. A. Chilla, Phys. Rev. Lett. **73**, 2192 (1994).
[11]G. Niimi, Y. Hayashi, N. Sakamoto, M. Nakajima, A. Okino, M. Watanabe, K. Horioka, and E. Hotta, IEEE Trans. Plasma Sci. **30**, 616 (2002).
[12]J. J. Rocca, Rev. Sci. Instrum. **70**, 3799 (1999).
[13]A. Ritucci, G. Tomassetti, A. Reale, F. Flora, and L. Mezi, Opt. Commun. **231**(1–6), 403 (2004).
[14]T. Hosokai, M. Nakajima, T. Aoki, M. Ogawa, and K. Horioka, Jpn. J. Appl. Phys., Part 1 **36**, 2327 (1997).
[15]J. Rocca, M. C. Marconi, and F. G. Tomasel, IEEE J. Quantum Electron. **29**, 182 (1993).
[16]H. J. Shin, D. E. Kim, and T. N. Lee, Phys. Rev. Lett. E **50**, 1376 (1994), available at http://pre.aps.org/abstract/PRE/v50/i2/p1376_1.
[17]J. J. Rocca, J. L. A. Chilla, S. Sakadzic, A. Rahman, J. Filevich, E. Jankowska, E. C. Hammarsten, and B. Luther, Proc. SPIE **4505**, 1 (2001).
[18]S. S. Ellwi, Z. Andrei, S. Plesli, and H. J. Kunze, Phys. Lett. A **292**, 125 (2001).
[19]K. Lee, J. H. Kim, and D. Kim, Phys. Plasmas **9**, 4749 (2002).
[20]P. Vrba, M. Vrbova, N. Dezhda, A. Bobrova, and P. V. Sasorov, Cent. Eur. J. Phys. **3**, 564 (2005).
[21]S. Kampel, A. Rikanati, I. Be'ery, A. Ben-Kish, A. Fisher, and A. Ron, Phys. Rev. E **78**, 056404 (2008).
[22]Y. Sakai, S. Takahashi, T. Hosokai, M. Watanabe, G. H. Kim, and E. Hotta, J. Appl. Phys. **107**, 083303 (2010).
[23]Y. Sakai, T. Komatsu, I. Song, M. Watanabe, G. H. Kim, and E. Hotta, Rev. Sci. Instrum. **81**, 013303 (2010).
[24]Y. Sakai, S. Takahashi, M. Watanabe, G. H. Kim, and E. Hotta, Rev. Sci. Instrum. **81**, 043504 (2010).
[25]H. R. Griem, *Plasma Spectroscopy* (McGraw-Hill, 1964).
[26]Saltzman, *Atomic Physics in Hot Plasmas* (Oxford University Press, 1997).
[27]H. Kumai, Y. Ishizuka, M. Watanabe, and E. Hotta, in *Proceedings of Physics and Application of Plasma Based on Pulsed Power Technology, Research Report NIFS-Proceedings Series, NIFS-PROC-90* (2012), pp. 67–72.
[28]M. Benk, K. Bergmann, D. Schäfer, and T. Wilhein, Opt. Lett. **33**(20) 2359–2361 (2008).
[29]K. Sawada and T. Fujimoto, Phys. Rev. E **49**, 5565 (1994).
[30]T. Holstein, Phys. Rev. **72**(12), 1212 (1947).
[31]M. Masnavi, M. Nakajima, and K. Horioka, IEEJ Trans. Fundam. Mater. **126**, 250 (2006).
[32]M. J. Seaton, Review of Atomic Collision Processes, in Proceedings from IAU Symposium No. 34 (1967), p. 129.
[33]T. Ozawa, S. Yamamura, N. Tatsumura, K. Horioka, and T. Kawamura, Phys. Plasmas **19**, 063302 (2012).